

## RESEARCH ARTICLE

# Identification of Hexahydrocannabiphorol Metabolites in Human Urine

Willi Schirmer<sup>1,2</sup>  | Stefan Schürch<sup>2</sup>  | Wolfgang Weinmann<sup>1</sup> <sup>1</sup>Institute of Forensic Medicine, Forensic Toxicology and Chemistry, University of Bern, Bern, Switzerland | <sup>2</sup>Department of Chemistry, Biochemistry and Pharmaceutical Sciences, University of Bern, Bern, Switzerland**Correspondence:** Willi Schirmer ([willi.schirmer@irm.unibe.ch](mailto:willi.schirmer@irm.unibe.ch))**Received:** 4 October 2024 | **Revised:** 10 February 2025 | **Accepted:** 13 February 2025

## ABSTRACT

Hexahydrocannabiphorol (HHCP) is an emerging semisynthetic cannabinoid, which has been known since 1942 from research of tetrahydrocannabinol (THC) analogs and homologs. After the ban of hexahydrocannabinol (HHC) in many European Countries HHCP emerged as a replacement among other similar compounds. First countries already placed HHCP under their narcotic substance law. The aim of this research was to identify human Phase I and II metabolites in urine after oral HHCP consumption. Enzymatic immunoassays of urine samples were tested negative for cannabinoids after a single oral consumption of 4-mg HHCP from a  $\Delta^9$ -THC abstinent volunteer. The HHCP sample consumed in the self-experiment was purchased from an online store and analyzed beforehand using GC–MS. LC–HR-MS/MS and GC–MS after derivatization were used for the identification of metabolites. Hydroxylated metabolites were found with hydroxylation on the side chain or on the alicyclic part of the molecule. Bishydroxylated HHCP metabolites were found in similar abundance as the monohydroxy metabolites. All of the bishydroxylated metabolites besides a minor metabolite had a hydroxyl group on the side chain and another hydroxyl group on the alicyclic part of the molecule. In addition, the corresponding glucuronides were identified by LC–HR-MS/MS. The exact positions and stereochemistry of the hydroxylation sites could not be determined. Due to the extensive metabolism of HHCP and the lacking cross-reactivity of urine samples after consumption in  $\Delta^9$ -THC specific immunoassays, it is recommended to include HHCP metabolites in routine screening methods. Monohydroxylated and bishydroxylated metabolites of HHCP and their respective glucuronides are suggested as forensic targets.

## 1 | Introduction

In 2022, a new class of new psychoactive substances with cannabinimetic effects emerged on the recreational market. These compounds are structurally related to  $\Delta^9$ -tetrahydrocannabinol, the main psychoactive compound found in *Cannabis sativa* L. The first entries were synthesized from THC or cannabidiol (CBD), and these class of NPS are therefore known as semisynthetic cannabinoids. This terminology also remained for cannabinimetics, which are not synthesized from THC or CBD but share structural features with them [1, 2].

One of this synthetically made cannabinoids is hexahydrocannabiphorol (HHCP), which is found as an epimeric mixture of (9*R*)-HHCP and (9*S*)-HHCP in recreational products. As other semisynthetic cannabinoids, HHCP is sold as a legal and psychoactive alternative in countries that placed *Cannabis* and its psychoactive component THC under their narcotic substance law. Until the ban of hexahydrocannabinol (HHC) on March 31, 2023, HHCP was not widely used in Switzerland. This changed immediately after HHC was banned. In response to the market, a class wide ban on dibenzopyran cannabinoids, including HHCP, was enacted on October 9, 2023 [3].

According to anecdotal reports from users, HHCP is more potent and longer lasting than HHC or THC. Two recent cases from HHCP intoxications were reported but no fatalities. In both cases, the patients were hospitalized for several days after intoxication [4, 5]. The strong and enduring intoxication poses a safety risk for the consumers. The potency of the HHCP epimers were just recently investigated. Janssens et al. used a  $\beta$ -arrestin2 recruitment assay and Persson et al. used a G-protein coupled receptor functional assay [6, 7]. They reported that (9R)-HHCP is the more active epimer.

In contrast to HHC, HHCP cannot be synthesized from CBD even though various vendors from online shops claim that. GC-MS analysis of recreationally used HHCP shows many substances with the same molecular ion and fragment ions as HHCP. Probably resulting from stereoisomers and regioisomers during synthesis [2, 8, 9]. The poor manufacturing process and lacking quality standard of HHCP and similar semisynthetic cannabinoids, which do not derive from CBD poses a further risk to consumers.

To date, no method has been published that can detect HHCP and in particular its metabolites. Urine samples are usually measured beforehand using enzymatic immunoassay. From urine samples after the consumption of HHC is known that they show false positive signals for THC, probably due to structural similarities of the HHC and THC metabolites [10–15]. A study that evaluated cross-reactivity of 24 dibenzopyran cannabinoids in whole blood showed that the cross-reactivity of THC derivatives decline with the chain length. (9R)-HHCP and (9S)-HHCP were tested positive at 500 ng/mL but not at the next lower concentration of 20 ng/mL or below. An ELISA test kit from Immunalysis for THC and metabolites was used [16]. Another study compared the cross-reactivity of THC derivatives with different immunological screening tests in various biological matrices and showed no positive results for the HHCP epimers at a concentration of 250 ng/mL. In both studies, potential HHCP metabolites were not included [11, 16]. To the authors knowledge, no potential metabolites of the HHCP epimers are commercially available.

As to date, only a single study reported potential metabolites of (9R)-HHCP and (9R)-HHCP-O (HHCP acetate) from incubation experiments with human hepatocytes. They concluded that differentiation between HHCP and HHCP-O consumption is unlikely because ester hydrolysis of HHCP-O to HHCP occurs rapidly. Reported metabolic reactions of (9R)-HHCP in the incubation experiments were monohydroxylation, bishydroxylation, bishydroxylation with dehydrogenation (oxo-alcohols and carboxylic acids), trihydroxylation with dehydrogenation, and subsequent glucuronidation [17]. These reported HHCP metabolites are likely found in *in vivo* samples after the consumption of HHCP.

The presented study aimed to identify the metabolites of the semisynthetic cannabinoid HHCP in urine. A routine LC-QqTOF screening method was used for the determination of the metabolites and their fragments. With this routine method, not all of the isomeric metabolites could be resolved; therefore, a LC-QqLIT was developed for the separation. Additionally, a GC-MS method was developed for the identification of potential

metabolic markers after derivatization with *N*-methyl-*N*-trimethylsilyltrifluoroacetamide (MSTFA).

## 1.1 | Chemicals and Reagents

HHCP was bought from a German online shop (47% (9R)-HHCP and 15% (9S)-HHCP, quantified by GC-MS (see Figure S1). Deionized water (18.2 M $\Omega$ -cm) was produced with a Milli-Q IQ 7000 system from Millipore (Billerica, MA, United States). Methanol (MeOH) ( $\geq 99.9\%$ ) was purchased from Carl Roth (Karlsruhe, Germany). Acetic acid (AcOH) (Reag. Ph. Eur.) and formic acid (50%, in water) were purchased from Grogg Chemie (Stettlen, Switzerland); *N*-methyl-*N*-trimethylsilyltrifluoroacetamide (MSTFA) ( $\geq 98.5\%$ ), *n*-butyl acetate (*n*-BuOAc) ( $\geq 99.7\%$ ), the alkane standard (C7–C40, 1000  $\mu$ g/mL), and ammonium formate ( $\geq 99.0\%$ ) were purchased from Sigma-Aldrich (Buchs, Switzerland). Acetonitrile (MeCN) ( $\geq 99.9\%$ ) was purchased from Thermo Fisher Scientific (Reinach, Switzerland). Chromabond C18 SPE cartridges (3 mL, 500 mg) were from Macherey-Nagel (Önsingen, Switzerland). The internal standards (ISTDs) (–)- $\Delta^9$ -*trans*-tetrahydrocannabinol- $D_3$  (THC- $D_3$ ), ( $\pm$ )-11-hydroxy- $\Delta^9$ -*trans*-tetrahydrocannabinol- $D_3$  (11-OH-THC- $D_3$ ), and ( $\pm$ )-11-nor-9-carboxy- $\Delta^9$ -*trans*-tetrahydrocannabinol- $D_3$  (THC-COOH- $D_3$ ) were purchased from Cerilliant (Round Rock, TX, United States). The reference standards (9R)-HHCP and (9S)-HHCP were purchased from Cayman Chemical (Ann Arbor, MI, United States). Instant buffer I and  $\beta$ -glucuronidase (BGTurbo) from Finden KURA was used. A homogenous enzyme immunoassay (HEIA) testkit 305UR for cannabinoids in urine from Immunalysis was used. The buffer solution, the  $\beta$ -glucuronidase, and the HEIA testkit 305UR were provided by Specialty Diagnostix (Passau, Germany). For the LC-QqLIT analysis, an ISTD solution was used which consisted of 0.1- $\mu$ g/mL THC- $D_3$ , 0.1- $\mu$ g/mL 11-OH-THC- $D_3$ , and 0.5- $\mu$ g/mL THC-COOH- $D_3$  in MeOH. A solution of MeCN in water (60%V) containing formic acid (0.1%V) was used for the sample reconstitution for LC-QqLIT and LC-QqTOF analysis.

### 1.1.1 | Recreational HHCP Product

The HHCP product for recreational use used in this study was analyzed in a previous study. Besides (9R)-HHCP and (9S)-HHCP, this sample contained unnatural regioisomers, unnatural stereoisomers, synthesis intermediates, and disubstituted heptylresorcinols from overalkylation. Five of the impurities and (9R)-HHCP were isolated, and their structure was elucidated with various NMR experiments. It was found that the (9R)-HHCP and (9S)-HHCP in this specific sample were enantiopure [9]. Both HHCP epimers were quantified in this recreational product using THC- $D_3$  as ISTD. The GC-MS method and instrument described in a previous publication was used [18]. This recreational HHCP product contained 47% (9R)-HHCP and 15% (9S)-HHCP by weight (see Figure S1).

### 1.1.2 | Self-Administration Experiment

In a self-experiment, a  $\Delta^9$ -THC abstinent volunteer ingested 4 mg of a well-characterized HHCP sample by dissolving it in olive oil

on an evening. Cannabimimetic effects started approximately 1 h after ingestion and lasted for approx. 10 h. Drowsiness, dizziness, and uncomfortable sleep were experienced. Full recovery was achieved 14 h after ingestion. An approval by an ethics committee is not required for self-experiments. Urine samples were collected before administration and for up to three days after ingestion. The metabolites were analyzed in the urine samples 10 and 15 h after ingestion. The first urine sample was collected 10 h after the HHCP ingestion.

## 1.2 | LC-QqTOF Analysis

The sample pretreatment was performed according to Schirmer et al. with slight modifications to the deglucuronidation step [10]. Briefly, 800- $\mu$ L urine, 20- $\mu$ L ISTD, 100- $\mu$ L instant buffer I, and 40- $\mu$ L  $\beta$ -glucuronidase solution were incubated at 50°C for 10 min. One-milliliter *n*-BuOAc was added; the mixture was shaken for 10 min and centrifuged for 10 min (13,000 rpm [17,190 $\times$ g], 8°C). Afterwards, the organic phase was transferred to an autosampler vial, evaporated to dryness under a stream of nitrogen at 50°C and reconstituted with 200- $\mu$ L reconstitution solution for further LC-MS analysis. For the analysis of the glucuronides, 800- $\mu$ L urine and 100- $\mu$ L ammonium formate solution (10 M, aq.) were mixed. The solution was extracted using 1 mL of cold MeCN. The organic phase was separated, evaporated to dryness, and the residue was dissolved in 200- $\mu$ L reconstitution solution. The same screening method with an LC-QqTOF instrument was used for the analysis as described previously. A Dionex Ultimate 3000 HPLC system (Thermo Fisher Scientific, Reinach, Switzerland) coupled to a TripleTOF 5600 mass spectrometer was used (Sciex, Toronto, Canada). Analyst TF software (Version 1.7) and Peak View (Version 1.2.0.3) (Sciex, Toronto, Canada) were used for data acquisition and processing. Mass spectra were measured in positive ionization mode with an IonDrive Turbo V ion source with TurboIonSpray probe. The curtain gas was set to 55.0 arbitrary units, the ion spray voltage floating was 5500 V, and the source temperature was 650°C. Ion Source Gases 1 and 2 were set to 55.0 arbitrary units. Chromatographic separation was performed on a Kinetex C8 column, 50 $\times$ 2.1 mm, 2.6  $\mu$ m, 100 Å (Phenomenex, Basel, Switzerland). A gradient method was used consisting of Mobile Phase A (0.1% aqueous formic acid [%V]) and Mobile Phase B (MeCN with 0.1% formic acid [%V]) with the following gradient: 2.5% B, 1–7 min: 2.5%–97.5% B, 7–11 min: 97.5% B, 11–11.1 min: 97.5%–2.5% B, 11.1–14 min: 2.5% B. The injection volume was 2.5  $\mu$ L, and the flow rate was 0.35 mL/min. The LC-QqTOF instrument was operated in information-dependent data acquisition (IDA) and in SWATH mode (sequential window acquisition of all theoretical mass spectra). For IDA a survey scan from *m/z* 100 to 950 was applied which triggered the acquisition of product ion mass spectra from *m/z* 50 to 950. For SWATH mode, a mass range from *m/z* 100 to 950 was scanned acquiring product ion spectra in windows of 35 Da from *m/z* 50 to 950. Collision energy with collision energy spread of 35  $\pm$  15 V was applied for IDA and SWATH acquisition.

## 1.3 | LC-QqLIT Analysis

Reference solutions were prepared by mixing 2  $\mu$ L of a 1- $\mu$ g/mL solution and 20- $\mu$ L ISTD. The solution was evaporated to dryness

and reconstituted in 200- $\mu$ L reconstitution solution. The extracts after deglucuronidation as described above were measured. A slightly changed protocol was used as described previously [10]. A Dionex Ultimate 3000 HPLC system (Thermo Fisher Scientific, Reinach, Switzerland) was used, coupled to a QTrap 4500 mass spectrometer (Sciex, Toronto, Canada) equipped with an IonDrive Turbo V ion source with TurboIonSpray probe. The curtain gas was set to 35.0 arbitrary units, the ion spray voltage was 4500 V, and the source temperature was 600°C. Ion Source Gases 1 and 2 were set to 40.0 arbitrary units. Data were acquired and processed with Analyst TF software (Version 1.7) and visualized with Sciex OS (Version 2.0.0.45330) (Sciex, Toronto, Canada). Chromatographic separation was performed on a Luna Omega PS C18 column, 100 $\times$ 2.1 mm, 1.6  $\mu$ m, 100 Å (Phenomenex, Basel, Switzerland). A gradient method was used consisting of Mobile Phase A (0.1% aqueous formic acid [%V]) and Mobile Phase B (MeCN with 0.1% formic acid [%V]) with the following gradient: 0–25 min: 35%–60% B, 25.1–39 min: 70% B, 39.1–41 min: 97.5% B, 41–41.1 min: 35% B. A flow rate of 0.4 mL/min and a column oven temperature of 40°C were applied. The injection volume was 1  $\mu$ L. Spectra were acquired in positive ionization mode with a multiexperimental method involving multiple reaction monitoring (MRM) and two product ion scans in “enhanced product ion” (EPI) mode. The product ion scans of the precursors ion with *m/z* 361.2 and 377.3 were acquired from *m/z* 50 to 380 with a scan rate of 10,000 Da/s, a declustering potential of 120 V, an entry potential of 10 V, and a collision energy of 35 V were applied. The relevant transitions with corresponding potentials of the MRM method are shown in Table 1

## 1.4 | GC-MS Analysis

For measurement of the reference spectra, 50  $\mu$ L of reference solutions ( $\gamma$  = 10  $\mu$ g/mL) was evaporated to dryness under a stream of nitrogen. The residue was dissolved in 25- $\mu$ L MSTFA and 25- $\mu$ L EtOAc. The mixture was then heated to 90°C for 40 min; 1  $\mu$ L of this solution was injected for GC-MS analysis. For measurement of sample solutions 1-mL urine, 200- $\mu$ L instant buffer I and 50- $\mu$ L  $\beta$ -glucuronidase (BGTurbo) were mixed and heated at 50°C for 15 min. The mixture was extracted with 500- $\mu$ L *n*-BuOAc by shaking for 10 min and centrifuging for 10 min (13,000 rpm [17,190 $\times$ g], 8°C). After separation, the organic phase was collected, and the extraction of the aqueous phase was repeated with 500- $\mu$ L *n*-BuOAc. The organic phases were combined and evaporated to dryness under a stream of nitrogen at 50°C. The residue was dissolved in 1-mL MeCN and diluted with 2-mL water. The residue was further purified by solid-phase extraction on a VacMaster 20 (Biotage, Uppsala, Sweden). Conditioning of the C18 SPE cartridges was achieved with 2-mL MeOH and 2-mL AcOH (0.1 M) prior to loading the sample solution (3 mL) onto the C18 cartridges. After loading, the cartridges were washed with 1-mL AcOH (0.1 M), 1-mL aqueous MeCN (40%V), and 1-mL aqueous MeCN (70%V). The samples were eluted using 1.5-mL MeCN. The eluate was transferred to an autosampler vial, evaporated to dryness under a stream of nitrogen at 70°C, redissolved in 25- $\mu$ L EtOAc and 25- $\mu$ L MSTFA and heated at 90°C for 40 min. One microliter of this solution was injected for GC-MS analysis.

**TABLE 1** | MRM transitions of the LC-QqLIT method.

Q1 (Da)	Q3 (Da)	DP (V)	CE (V)	CXP (V)	Name
334.2	316.2	87	21	12	11-OH-THC-D <sub>3</sub> MRM1
334.2	196.2	90	35	7	11-OH-THC-D <sub>3</sub> MRM2
348.2	330.2	93	23	12	THC-COOH-D <sub>3</sub> MRM1
348.2	302.2	102	28	12	THC-COOH-D <sub>3</sub> MRM2
318.2	196.3	88	32	7	THC-D <sub>3</sub> MRM 1
318.2	123.0	100	43	8	THC-D <sub>3</sub> MRM 2
345.3	221.2	88	32	7	HHCP MRM 1
345.3	123.0	100	43	8	HHCP MRM 2
361.3	343.3	87	21	12	OH-HHCP MRM1
361.3	221.2	90	35	7	OH-HHCP MRM2
361.3	219.1	90	35	7	OH-HHCP MRM3
377.3	359.3	87	21	12	2OH-HHCP MRM1
377.3	341.3	90	35	7	2OH-HHCP MRM2
377.3	219.1	90	35	7	2OH-HHCP MRM3

Note: A dwell time of 20 ms for every transition was applied. Abbreviations: CE: collision energy, CXP: cell exit potential, DP: declustering potential.

The samples were analyzed on an 8890 gas chromatograph with a 7693A autosampler coupled to a 5977B mass selective detector (Agilent, Basel, Switzerland). Data were acquired with MassHunter Workstation GC/MS Data Acquisition (Version 10.1.49) and analyzed with Enhanced ChemStation (F.01.03.2357) (Agilent). Chromatographic separation was performed on a 5% phenylmethylsiloxane column (HP-5ms Ultra Inert, 30 m, 250  $\mu$ m i.d., 0.25- $\mu$ m film thickness; Agilent J&W). Helium with a constant flow of 1 mL/min was used as a carrier gas. Chromatography occurred in pulsed splitless mode; injection volume was 1  $\mu$ L. The oven temperature was set to 80°C at the beginning and was ramped with 10°C/min to 300°C and held for 1 min, resulting in a total separation time of 23 min. The quadrupole temperature was set to 150°C, and the source

temperature to 230°C. The mass spectra (electron impact) were obtained with an ionization energy of 70 eV. The scan range was from  $m/z$  40 to 650 with a scan speed of 1.562 s<sup>-1</sup>.

## 1.5 | Fragmentation Behavior of HHCP and Metabolites

The product ion spectrum of HHCP shows fragment ions, which are characteristic for cannabinoids. Figure 1 shows the MS/MS spectrum of (9R)-HHCP. The epimer (9S)-HHCP shows the same spectrum (spectrum found in Figure S2).

The fragments can be divided into those that originate from the alicyclic part or from the aromatic part of the molecule. Hydroxylated HHCP show similar fragment ions to HHCP, which are shifted by +16 Da. Often only the dehydrated fragment ion is visible in the spectrum (shifted by -2 Da). Occurrence of the shifted fragments allows the determination of the hydroxylation position.

### 1.5.1 | Fragment Ions From the Alicyclic Part

The fragment ions  $m/z$  137,  $m/z$  95, and  $m/z$  81 originate from the alicyclic moiety as shown in Figure 1. Hydroxylation on this part leads to the fragment ions  $m/z$  153 and  $m/z$  135.

### 1.5.2 | Fragment Ions From the Aromatic Part

The fragment ion  $m/z$  289 is formed after elimination of *isobutene*, it is barely visible. The dihydrochromenylium ion  $m/z$  261 is low abundant as well. An ion with the same  $m/z$  ( $m/z$  261) might also result from the McLafferty rearrangement on the side chain. The fragment  $m/z$  221 is the main fragment ion of HHCP. The resulting benzylium/tropylium ion is very stable. Occurrence of the ion  $m/z$  219 in similar abundance is an indicator for side-chain substitution, especially when its hydrate, the ion  $m/z$  237, is still visible. Absence of the ion  $m/z$  123 and the simultaneous presence of  $m/z$  139 allows determining hydroxylations on the aromatic positions.

## 2 | Results

Urine samples of a volunteer who orally ingested 4 mg of HHCP were negative in immunoassays for THC and metabolites. This could be explained by poor cross-reactivity for longer alkyl chain dibenzopyran cannabinoids and their metabolites in immunoassays designed for THC and THC metabolites.

LC-QqTOF, LC-QqLIT, and GC-MS were used for metabolite identification. For the rapid in-house LC-QqTOF screening method, the urine samples were measured after and prior deglucuronidation for the identification of Phase I and Phase II metabolites. Phase I metabolites were bishydroxylated metabolites of HHCP (M1–M4) and monohydroxylated metabolites (M5 and M6). Phase II metabolites consisted of HHCP glucuronide, the glucuronides of bishydroxylated HHCP (M7–M10), and the glucuronides of bishydroxylated HHCP (M11–M13). Fragmentation

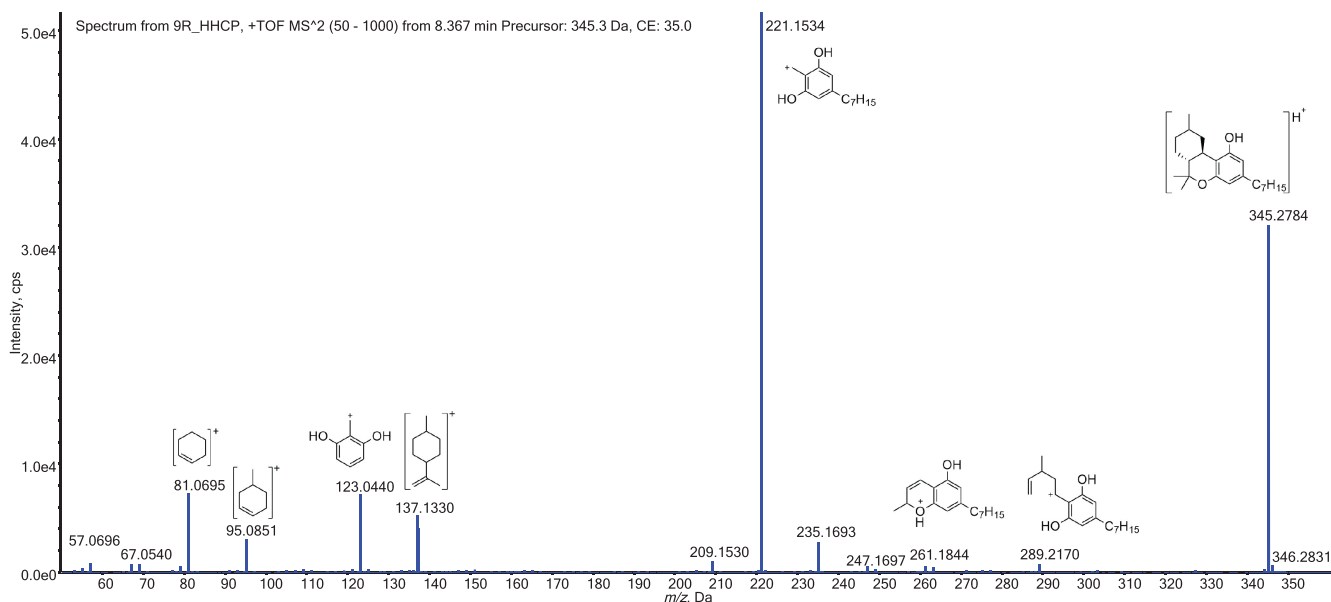


**FIGURE 1** | Product ion spectrum of (9R)-HHCP.

patterns were elucidated from the exact masses of the molecular ions and fragments. They are similar to the patterns found in HHC and its respective metabolites. Metabolite coelution was an issue with this rapid screening method and therefore a LC-QqLIT method with a slower gradient was developed to separate Phase I metabolites.

In the LC-QqLIT method, bishydroxylated metabolites (M14–M17), monohydroxylated metabolites (M18–M21), and slight amounts of HHCP were detected. No carboxylated metabolites were found. Product ion spectra were acquired in EPI mode, and an MRM method was used for sensitive detection.

Additionally, a GC–MS method after derivatization of the metabolites was developed. The fragmentation mechanisms of dibenzopyran cannabinoids and their trimethylsilyl ethers with a similar structure to HHCP have been investigated thoroughly. HHCP and carboxylated metabolites were not detected. A monohydroxylated metabolite of HHCP was detected, which was tentatively identified as (9R)-11-OH-HHCP. Additionally, two bishydroxylated metabolites were detected.

The monohydroxylated metabolites were either hydroxylated on the alicyclic part or on the heptyl chain of HHCP. The bishydroxylated metabolites were hydroxylated once on the alicyclic part and once on the heptyl chain of HHCP, the minor metabolite M9 was an exception, and this bishydroxylated metabolite had two hydroxylation positions on the alicyclic moiety of HHCP. Their fragmentational behavior is explained later in the text.

## 2.1 | LC-QqTOF: Phase I Metabolites

After deglucuronidation of the urine samples, monohydroxylated and bishydroxylated metabolites of HHCP were found. HHCP was detected as well, but only in small quantities, which indicates a strong metabolization of HHCP. The chromatogram of a deglucuronidated urine sample is shown in Figure 2. A

chromatogram of a deglucuronidated urine sample before the ingestion of HHCP is found in Figure S3. Bishydroxylated HHCP (M1–M4) and hydroxylated HHCP (M5 and M6) were found in the sample but no carboxylated metabolites. The spectra of the metabolites M1–M6 are found in Figures S4–S8.

Three bishydroxylated metabolites of HHCP were identified with LC-QqTOF. The mass spectrum of metabolite M1 shows the protonated molecular ion  $[M+H]^+$  at  $m/z$  377.2686 ( $C_{23}H_{37}O_4^+$ ,  $-13.3$  ppm). The base peak is formed after loss of  $H_2O$  at  $m/z$  359.2581 ( $C_{23}H_{35}O_3^+$ ,  $-1.4$  ppm), a second loss of  $H_2O$  can be observed at  $m/z$  341.2475 ( $C_{23}H_{33}O_2^+$ ,  $-0.3$  ppm). The phenolic hydroxy group remains intact. The hydroxylated tropylium ion at  $m/z$  237.1485 ( $C_{14}H_{21}O_3^+$ ,  $1.7$  ppm) is present and so is the ion after dehydration at  $m/z$  219.1380 ( $C_{14}H_{19}O_2^+$ ,  $2.7$  ppm). The presence of these tropylium ions show that this metabolite is monohydroxylated at the side chain, the fragment ions are shown in Figure S37.

An ion with  $m/z$  285.1849 ( $C_{19}H_{25}O_2^+$ ,  $-2.8$  ppm) is present which forms after the loss of *iso*-butene and two  $H_2O$ , the respective hydrates ( $m/z$  303.1955 [ $C_{19}H_{27}O_3^+$ ] and  $m/z$  321.2060 [ $C_{19}H_{29}O_4^+$ ]) are not observed. The chromenylium ion  $m/z$  257.1536 ( $C_{17}H_{21}O_2^+$ ,  $7.0$  ppm) and its hydrate  $m/z$  275.1642 ( $C_{17}H_{23}O_3^+$ ,  $-7.3$  ppm) are characteristic ions. The presence of the ions  $m/z$  135.1168 ( $C_{10}H_{15}^+$ ,  $-11.8$  ppm) and its hydrate  $m/z$  153.1274 ( $C_{10}H_{17}O^+$ ,  $-12.4$  ppm), which originate from the alicyclic part, indicates a hydroxylation on that part. The ion  $m/z$  93.0699 ( $C_7H_9^+$ ,  $-12.9$  ppm), which originates from the alicyclic part, supports this. However, its hydrate ( $m/z$  111.0804 [ $C_7H_{11}O^+$ ]) was not detected.

Mass spectrum of metabolite M2 shows the same fragment ions but with different relative intensities, indicating that M2 is hydroxylated on the alicyclic part and on the heptyl group. The same is true for metabolite M3, which shows a similar mass spectrum. The bishydroxylated HHCP are all hydroxylated on the chain and the alicyclic moiety of the molecule. A mass spectrum for the metabolite M4 was only obtained from the SWATH

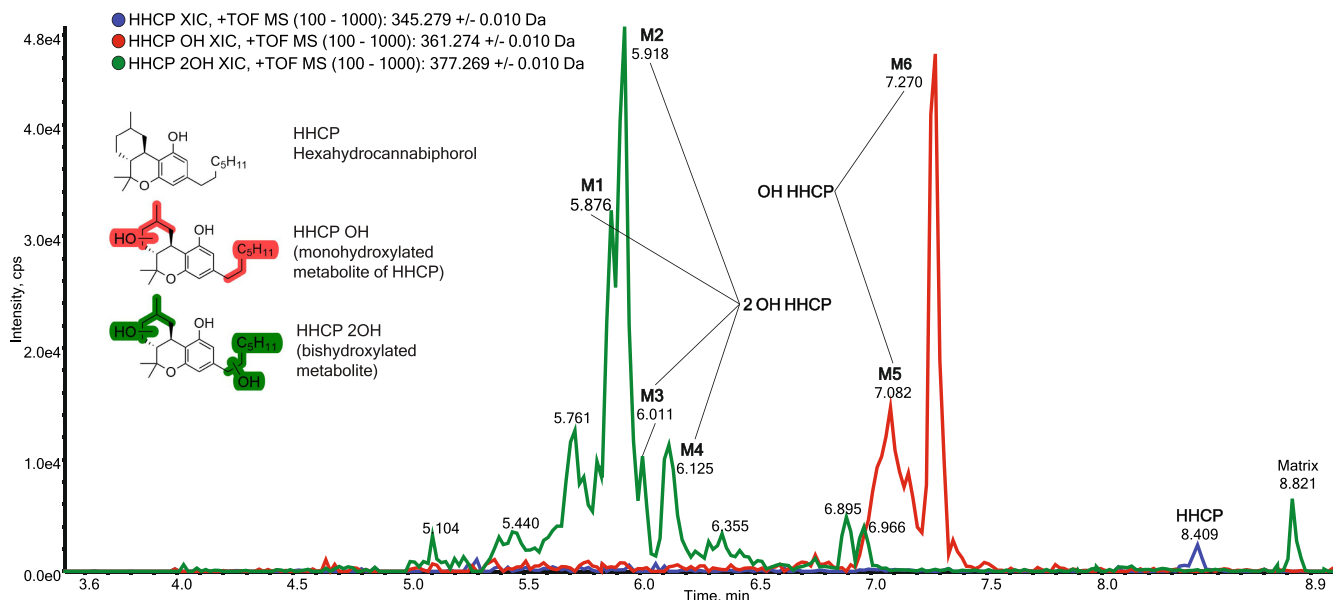


**FIGURE 2** | Extracted ion chromatograms of a deglucuronidated urine sample, 10h after oral ingestion of 4-mg HHCP. HHCP (blue), monohydroxylated HHCP (red), and bishydroxylated HHCP (green).

acquisition, the spectrum shows the same fragment ions as described for M1.

In the mass spectrum of the metabolite M5 a protonated molecular ion of  $m/z$  361.2737 ( $C_{23}H_{37}O_3^+$ ,  $-5.0$  ppm) can be observed. Loss of  $H_2O$  forms the base peak of this spectrum  $m/z$  343.2632 ( $C_{23}H_{35}O_2^+$ ,  $1.2$  ppm). An ion of  $m/z$  287.2006 ( $C_{19}H_{27}O_2^+$ ,  $4.5$  ppm) is present which is formed after the loss of *iso*-butene and  $H_2O$ . The ion at  $m/z$  259.1693 ( $C_{17}H_{23}O_2^+$ ,  $-15.0$  ppm) might be a dihydrochromenylium ion with an unsaturated side chain or the product after McLafferty rearrangement and loss of  $H_2O$ . The respective hydrates ( $m/z$  277.1789 [ $C_{17}H_{25}O_3^+$ ]) are not observed. The ion  $m/z$  123.0441 ( $C_7H_7O_2^+$ ,  $-8.1$  ppm) is also seen for HHCP. The ions  $m/z$  221.1536 ( $C_{14}H_{21}O_2^+$ ,  $-21.3$  ppm),  $m/z$  135.1168 ( $C_{10}H_{15}^+$ ,  $-21.5$  ppm), and  $m/z$  93.0699 ( $C_7H_9^+$ ,  $-24.7$  ppm) are observed which might be the fragments of a metabolite which is hydroxylated on the alicyclic moiety. In addition, the ions  $m/z$  219.1380 ( $C_{14}H_{19}O_2^+$ ,  $-5.9$  ppm),  $m/z$  137.1325 ( $C_{10}H_{17}^+$ ,  $1.5$  ppm), and  $m/z$  95.0855 ( $C_7H_{11}^+$ ,  $0.0$  ppm) can be observed in the mass spectrum. These are likely fragments of a metabolite, which is hydroxylated on the side chain. The characteristic fragment ions are shown in Figure S38. Coelution of side-chain hydroxylated and alicyclic hydroxylated metabolites would explain the presence of all the ions observed in this mass spectrum. The chromatogram shown in Figure 2 does not show well-separated peaks, and coelution of several monohydroxylated and bishydroxylated metabolites is assumed.

The mass spectrum of M6 shows the protonated molecular ion of  $m/z$  361.2737 ( $C_{23}H_{37}O_3^+$ ,  $-1.1$  ppm). Loss of  $H_2O$  leads to an ion of  $m/z$  343.2632 ( $C_{23}H_{35}O_2^+$ ,  $0.6$  ppm). An ion of  $m/z$  287.2006 ( $C_{19}H_{27}O_2^+$ ,  $-3.5$  ppm) is observed which forms after fragmentation of *iso*-butene and  $H_2O$ . The dihydrochromenylium ion of  $m/z$  261.1849 ( $C_{17}H_{25}O_2^+$ ,  $-13.4$  ppm) is observable. Base peak of this spectrum is the tropylium ion  $m/z$  221.1536 ( $C_{14}H_{21}O_2^+$ ,  $-3.2$  ppm). It indicates that this molecule has no hydroxyl group on the side chain. This can also be seen from the fragments

resulting from the fragmentation of the alicyclic part  $m/z$  93.0699 ( $C_7H_9^+$ ,  $0.0$  ppm) and  $m/z$  135.1168 ( $C_{10}H_{15}^+$ ,  $-9.6$  ppm); the respective hydrates ( $m/z$  111.0804 [ $C_7H_{11}O^+$ ] and  $m/z$  153.1274 [ $C_{10}H_{17}O_2^+$ ]) are not observed. The dihydrochromenylium ion of  $m/z$  261.1849 ( $C_{17}H_{25}O_2^+$ ) allows determining the hydroxylation position of this molecule even narrower at positions C6a, C7, or C8. Positions C7 and C8 seem more likely. The characteristic ions are shown in Figure S39. Metabolic hydroxylation at the *gem*-dimethyl carbons (C12 or C13) of similar compounds were only observed for abnormal cannabinoids. Brown and Harvey found hydroxylation at these positions in mouse liver after application of *abn*- $\Delta^8$ -THC-C1 [19].

## 2.2 | LC-QqTOF: Phase II Metabolites

Extracted ion chromatograms of a urine sample 10h after the ingestion of 4-mg HHCP, which was not treated with  $\beta$ -glucuronidase shows HHCP, four bishydroxylated HHCP (M7–M10), and three hydroxylated HHCP (M11–M13) as their glucuronides as seen in Figure 3. A chromatogram with the same traces from a urine sample before the self-experiment is found in Figure S9.

Protonated HHCP glucuronide  $m/z$  521.3109 ( $C_{29}H_{45}O_8^+$ ,  $-5.0$  ppm) is detected at 7.05 min. The elimination of two  $H_2O$  molecules can be observed ( $m/z$  485.2898 [ $C_{29}H_{41}O_6^+$ ],  $7.6$  ppm), which is probably due to the dehydration of the glucuronide moiety. Base peak of this spectrum is the protonated HHCP of  $m/z$  345.2788 ( $C_{23}H_{37}O_2^+$ ,  $-3.5$  ppm), which forms after loss of dehydrated glucuronide. The same fragments with low  $m/z$  values as in HHCP are present but of lower abundance. These are the tropylium ion of  $m/z$  221.1536 ( $C_{14}H_{21}O_2^+$ ,  $-14.5$  ppm), the methyl-isopropenyl disubstituted cyclohexylium ion ( $m/z$  137.1325 [ $C_{10}H_{17}^+$ ],  $-11.7$  ppm), and the methylcyclohexenylium ion ( $m/z$  95.0855 [ $C_7H_{11}^+$ ],  $-12.6$  ppm). The corresponding spectrum is found in Figure S10.

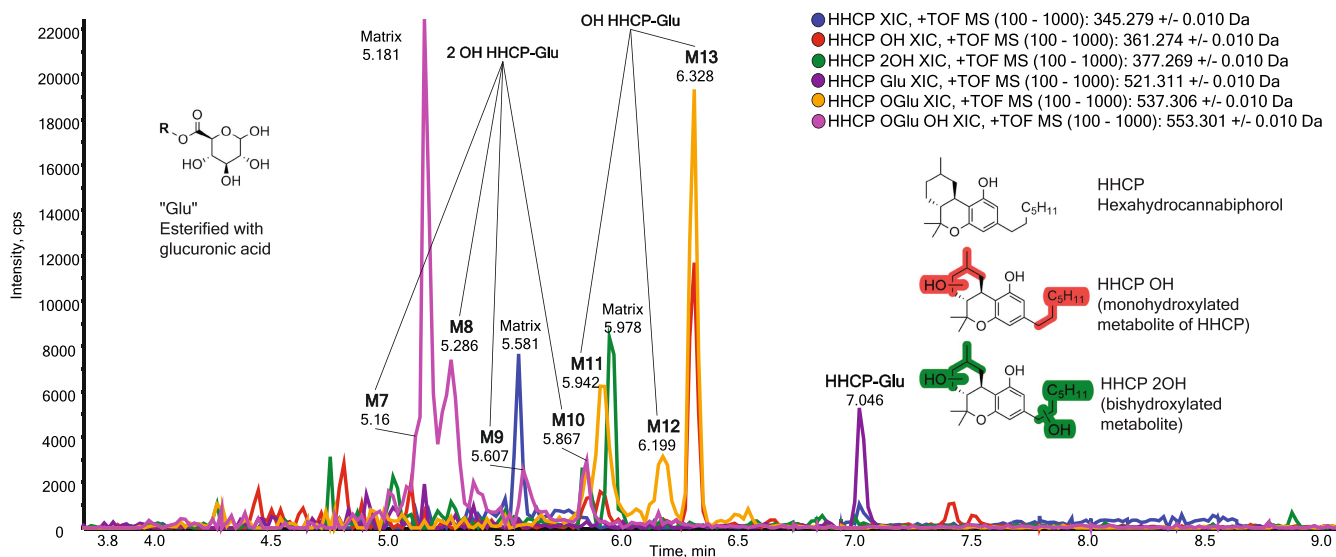


**FIGURE 3** | Extracted ion chromatograms in an untreated urine sample, 10h after oral consumption of 4-mg HHCP. HHCP (blue), HHCP glucuronide (purple, HHCP Glu), monohydroxylated HHCP (red, HHCP OH), monohydroxylated HHCP glucuronide (yellow, HHCP OGlu), bishydroxylated HHCP (green, HHCP 2OH), and bishydroxylated HHCP glucuronide (pink, HHCP OGlu OH). Peaks at 5.18 (purple), 5.58 (blue), and 5.98 min (green) also appear in a urine sample before the ingestion of HHCP.

Four metabolites (M7–M10) were detected that are likely bishydroxylated HHCP glucuronides (spectra found in Figures S11–S14). The mass spectrum of M7 shows a very abundant molecular ion as base peak ( $m/z$  553.3007 [ $C_{29}H_{45}O_{10}^+$ ],  $-9.4$  ppm). After loss of the glucuronide moiety, a protonated bishydroxylated HHCP ( $m/z$  377.2686 [ $C_{23}H_{37}O_4^+$ ],  $-51.4$  ppm) remains. Its anhydrate  $m/z$  359.2581 ( $C_{23}H_{35}O_3^+$ ,  $-24.2$  ppm) is also present, resulting from the loss of  $H_2O$ . The tropylium ion  $m/z$  219.1380 ( $C_{14}H_{19}O_2^+$ ,  $18.7$  ppm) is the only indicator that this metabolite is hydroxylated on the side chain and the alicyclic part.

A mass spectrum of the metabolite M8 was only obtained by SWATH acquisition mode. The characteristic ions are the molecular ion  $m/z$  553.3007 ( $C_{29}H_{45}O_{10}^+$ ,  $11.4$  ppm), loss of glucuronide  $m/z$  377.2686 ( $C_{23}H_{37}O_4^+$ ,  $4.2$  ppm), loss of glucuronide and  $H_2O$   $m/z$  359.2581 ( $C_{23}H_{35}O_3^+$ ,  $-7.5$  ppm), and the tropylium ion  $m/z$  219.1380 ( $C_{14}H_{19}O_2^+$ ,  $-11.9$  ppm), indicating that this metabolite is hydroxylated on the side chain and the alicyclic part.

The mass spectrum of the minor metabolite M9 shows the molecular ion  $m/z$  553.3007 ( $C_{23}H_{37}O_4^+$ ,  $58.4$  ppm), loss of glucuronide  $m/z$  377.2686 ( $C_{23}H_{37}O_4^+$ ,  $0.0$  ppm), loss of glucuronide and  $H_2O$   $m/z$  359.2581 ( $C_{23}H_{35}O_3^+$ ,  $-14.2$  ppm), further loss of  $H_2O$   $m/z$  341.2475 ( $C_{23}H_{33}O_2^+$ ,  $48.6$  ppm), and the tropylium ion  $m/z$  221.1536 ( $C_{14}H_{21}O_2^+$ ,  $-1.8$  ppm). This metabolite is bishydroxylated on the alicyclic part.

The mass spectrum of the minor metabolite M10 shows the molecular ion  $m/z$  553.3007 ( $C_{23}H_{37}O_4^+$ ,  $-19.5$  ppm). Base peak of the spectrum is a protonated bishydroxy-HHCP of  $m/z$  377.2686 ( $C_{23}H_{37}O_4^+$ ,  $2.9$  ppm). Dehydration of the base peak might be present, an ion of  $m/z$  359.2581 ( $C_{23}H_{35}O_3^+$ ,  $-26.7$  ppm) is observed. The tropylium ion with a hydroxyl group on the side chain is observable ( $m/z$  237.1485 [ $C_{14}H_{21}O_3^+$ ],  $-10.1$  ppm). Interestingly, the dehydrated tropylium ion  $m/z$  219.1380 ( $C_{14}H_{19}O_2^+$ ) was not observed. This metabolite possesses a hydroxy group on the side chain and another one on the alicyclic moiety of the molecule.

The hydroxylated HHCP glucuronides are found at retention times of 5.94 (M11), 6.20 (M12), and 6.33 min (M13) (spectra are found in Figures S15–S18). Mass spectrum of the metabolite M12 shows a quite intensive protonated molecular ion of  $m/z$  537.3058 ( $C_{29}H_{45}O_9^+$ ,  $-6.7$  ppm). Three losses of  $H_2O$  are observed ( $m/z$  519.2952 [ $C_{29}H_{43}O_8^+$ ],  $3.5$  ppm;  $m/z$  501.2831 [ $C_{29}H_{41}O_7^+$ ],  $-3.2$  ppm; and  $m/z$  483.2774 [ $C_{29}H_{39}O_6^+$ ],  $6.8$  ppm). Protonated monohydroxy HHCP ( $m/z$  361.2737 [ $C_{23}H_{37}O_3^+$ ],  $-6.6$  ppm) and its anhydrate ( $m/z$  343.2632 [ $C_{23}H_{35}O_2^+$ ],  $-0.9$  ppm) are present, the latter forms the base peak of the spectrum. The ions  $m/z$  287.2006 ( $C_{19}H_{27}O_2^+$ ,  $0.0$  ppm),  $m/z$  259.1693 ( $C_{17}H_{23}O_2^+$ ,  $-7.3$  ppm),  $m/z$  221.1536 ( $C_{14}H_{21}O_2^+$ ,  $-5.0$  ppm), and  $m/z$  135.1168 ( $C_{10}H_{15}^+$ ,  $-3.7$  ppm) indicate a metabolite with hydroxylation on the alicyclic moiety. But the ions  $m/z$  261.1849 ( $C_{17}H_{25}O_2^+$ ,  $16.5$  ppm),  $m/z$  219.1380 ( $C_{14}H_{19}O_2^+$ ,  $-4.6$  ppm), and  $m/z$  137.1325 ( $C_{10}H_{17}^+$ ,  $4.4$  ppm), which indicate a side-chain hydroxylated metabolite, are also present. Coelution of metabolites would explain this finding.

Mass spectrum of the metabolite M13 shows the protonated molecular ion of  $m/z$  537.3058 ( $C_{29}H_{45}O_9^+$ ,  $11.9$  ppm). Protonated monohydroxy HHCP ( $m/z$  361.2737 [ $C_{23}H_{37}O_3^+$ ],  $-6.4$  ppm) forms the base peak of this spectrum. The tropylium ion ( $m/z$  221.1536 [ $C_{14}H_{21}O_2^+$ ],  $8.1$  ppm), the hydroxycyclohexylium ion ( $m/z$  153.1274 [ $C_{10}H_{17}O^+$ ],  $-4.6$  ppm), and its anhydrate ( $m/z$  135.1168 [ $C_{10}H_{15}^+$ ],  $14.1$  ppm) indicate that this metabolite is hydroxylated on the alicyclic part of the molecule. The ion  $m/z$  287.2006 ( $C_{19}H_{27}O_2^+$ ,  $2.8$  ppm), which forms after the elimination of *iso*-butene and  $H_2O$ , is of quite high intensity compared to the similar ion  $m/z$  289.2162 ( $C_{19}H_{29}O_2^+$ ) from the fragmentation of HHCP which indicates high stability due to conjugation of the ion.

The mass spectrum of the metabolite M10 also consists of coelution of side-chain hydroxylated and alicyclic hydroxylated HHCPs.

## 2.3 | LC-QqLIT Analysis

A chromatogram from the deglucuronidated urine sample 15 h after oral ingestion of 4-mg HHCP is shown in Figure 4. The chromatograms of the urine sample before and 10 h after the ingestion of HHCP are found in Figures S19 and S20. HHCP was barely detected after deglucuronidation (30.2 min). An intense metabolite with the transitions  $m/z$  361.3  $\rightarrow$   $m/z$  343.3 and  $m/z$  361.3  $\rightarrow$   $m/z$  221.2 is detected at 20.4 min. This compound is a monohydroxylated HHCP, which is hydroxylated at the alicyclic part. Several compounds with the transitions  $m/z$  361.3  $\rightarrow$   $m/z$  343.3 and either  $m/z$  361.3  $\rightarrow$   $m/z$  221.2 or  $m/z$  361.3  $\rightarrow$   $m/z$  219.1 are detected between 16.5 and 19.0 min, which are not baseline separated, indicating that several monohydroxylated species are formed during metabolism. Two intense metabolites with characteristic mass transitions of  $m/z$  377.3  $\rightarrow$   $m/z$  359.3 and  $m/z$  377.3  $\rightarrow$   $m/z$  219.1 are seen at 6.4 and 6.7 min, respectively. These correspond to bishydroxylated species. EPI spectra of the precursor  $m/z$  377.3 show the same ions as described in the LC-QqTOF analysis part.

## 2.4 | LC-QqLIT Bishydroxylated Metabolites

Four bishydroxylated metabolites (M14–M17) are found in the chromatogram at 4.9, 5.2, 6.4, and 6.8 min (mass spectra are included in Figures S21–S24). In addition, several minor metabolites are present, which might result from isomeric impurities of the ingested HHCP sample. The peak at 9.0 min results from the matrix, as it is also present in the urine sample collected before the self-administration of HHCP.

The product ion spectrum of M14 shows fragment ions, which seem to be not characteristic for bishydroxylated HHCP, this might be a bishydroxylated metabolite of an HHCP isomer which are present in the ingested HHCP sample. M15 shows a few characteristic ions but might also result from an isomer, the tropylium ion ( $m/z$  219) is also of a quite low abundance. The product ion spectra of the major metabolite M16 shows

the molecular ion ( $m/z$  377.13) as base peak. Two losses of  $H_2O$  can be observed ( $m/z$  359.22 and 341.25) which are the introduced hydroxyl groups. A very abundant tropylium ion with an unsaturated side chain is seen at  $m/z$  219.09. In addition, the chromenylium ion with an unsaturated side chain ( $m/z$  257.14) and its hydrate ( $m/z$  275.11) are present, confirming that a hydroxylation position is present on the side chain and another one on the alicyclic moiety of the metabolite. A product ion spectrum of M16 is depicted on Figure 5.

The product ion spectrum of M17 shows the molecular ion ( $m/z$  377.17). The tropylium ion ( $m/z$  219.19) indicates a hydroxylation position on the side chain and the fragment ion ( $m/z$  134.98) indicates a hydroxylation position on the alicyclic part of the molecule.

## 2.5 | LC-QqLIT Monohydroxylated Metabolites

The product ion spectrum of the metabolite M18 shows the ion  $m/z$  219 indicating a side-chain hydroxylated HHCP. In the product ion spectra of M19 and M20, no characteristic ions were identified; instead, other ions are found. These compounds are not found in the blank urine chromatogram and are therefore likely metabolites of HHCP isomers, which were present in the ingested sample. The product ion spectrum of M21 (Figure 6) shows a very abundant ion of  $m/z$  221. The metabolite M21 is likely (9*RS*)-11-OH-HHCP, as it shows a similar chromatographic behavior to the homologs (9*RS*)-11-OH-HHC [10]. It elutes after side-chain hydroxylated metabolites in similar chromatographic conditions. The major fragment ion is the tropylium ion  $m/z$  221 ( $m/z$  193 for the homolog (9*RS*)-11-OH-HHC), and the fragment ion after loss of water  $m/z$  343 ( $m/z$  315 for the homolog) is barely visible. The product ion spectrum is similar to the homolog (9*R*)-11-OH-HHC; the molecular ion ( $m/z$  361) and main fragment ions ( $m/z$  287,  $m/z$  235 and  $m/z$  221) are shifted by the mass of ethylene ( $C_2H_4$ , +28 Da). The product ion spectra of the metabolites M18–M21 are included in Figures S25–S28.

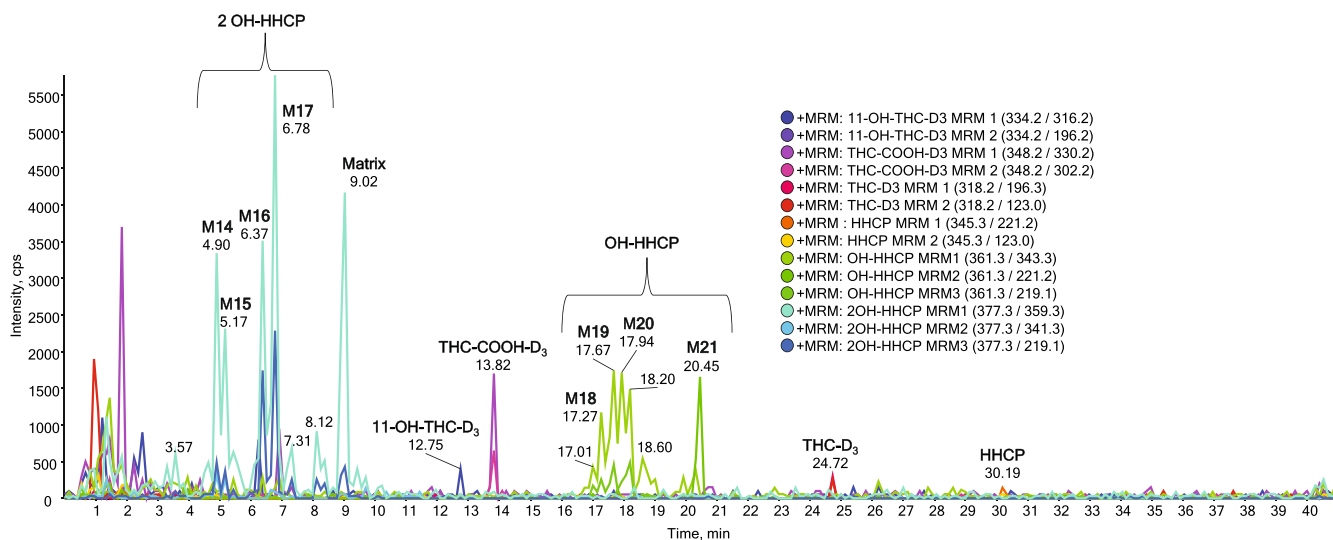


**FIGURE 4** | Extracted ion chromatograms for characteristic mass transitions of HHCP (yellow, orange), monohydroxylated HHCP (green shades) and dihydroxylated HHCP (cyan, blue). Chromatogram shows a deglucuronidated urine sample collected 15 h after oral ingestion of 4-mg HHCP.

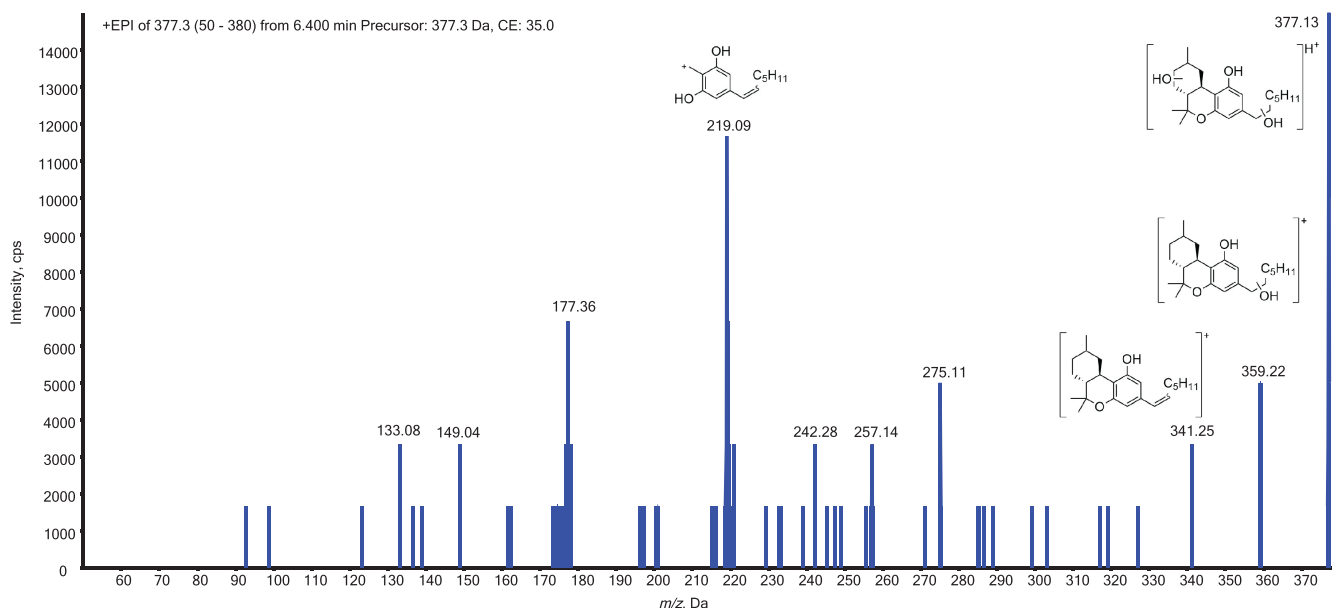


**FIGURE 5** | Product ion spectrum of the metabolite M16. A bishydroxylated metabolite of HHCP.

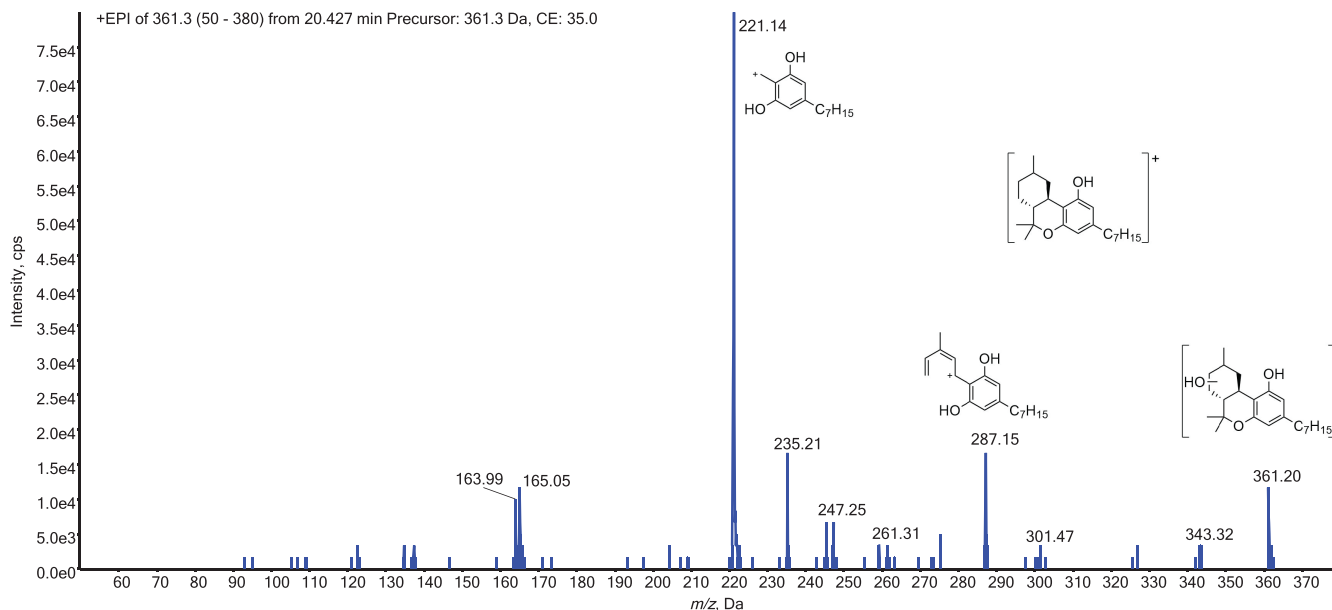


**FIGURE 6** | Product ion spectrum of the metabolite M21. Tentatively identified as (9*R*)-11-OH-HHCP.

## 2.6 | GC-MS of HHCP-TMS

The mass spectra of (9*R*)-HHCP and (9*S*)-HHCP are identical. Formation of the relevant ions were discussed previously [9]. Major ions are the molecular ion ( $[M]^+$ ,  $m/z$  344), loss of a propyl radical ( $[M-C_3H_7]^+$ ,  $m/z$  301), and the tropylium ion ( $[M-123]^+$ ,  $m/z$  221). Loss of *n*-hexene from a McLafferty rearrangement ( $[M-C_6H_{12}]^+$ ,  $m/z$  260) is the base peak of their spectra. The unnatural diastereomer *cis*-HHCP ((6*S*,9*R*,10*aR*)-configuration) shows the same mass spectrum [9].

Mass spectra of the trimethylsilylated (9*R*)- and (9*S*)-HHCP are indistinguishable. They show similar fragments with similar intensities as the underivatized samples but shifted by 72 Da ( $-H$ ,  $+Si(CH_3)_3$ ). The base peak is a radical cation with  $m/z$  332, which

results from the loss of *n*-hexene after McLafferty rearrangement. Loss of the methyl radical ( $[M-CH_3]^+$ ,  $m/z$  401) is more prominent than in the fragmentation of underivatized HHCP. The same fragmentation pathways are suggested as for underivatized HHCP and other well-characterized cannabinoids and their trimethylsilyl ethers [9, 20–23]. Figure 7 shows an EI mass spectrum of trimethylsilylated (9*S*)-HHCP. Spectra and XIC ( $m/z$  416) of (9*R*)- and (9*S*)-HHCP-TMS are included in Figures S29 and S30.

No HHCP-TMS was detected in the urine samples using this GC-MS method, indicating excessive metabolism of the parent compounds. Figure 8 shows that the derivatized urine sample, which was taken 10 h after oral ingestion of 4-mg HHCP, has no detectable amount of HHCP.

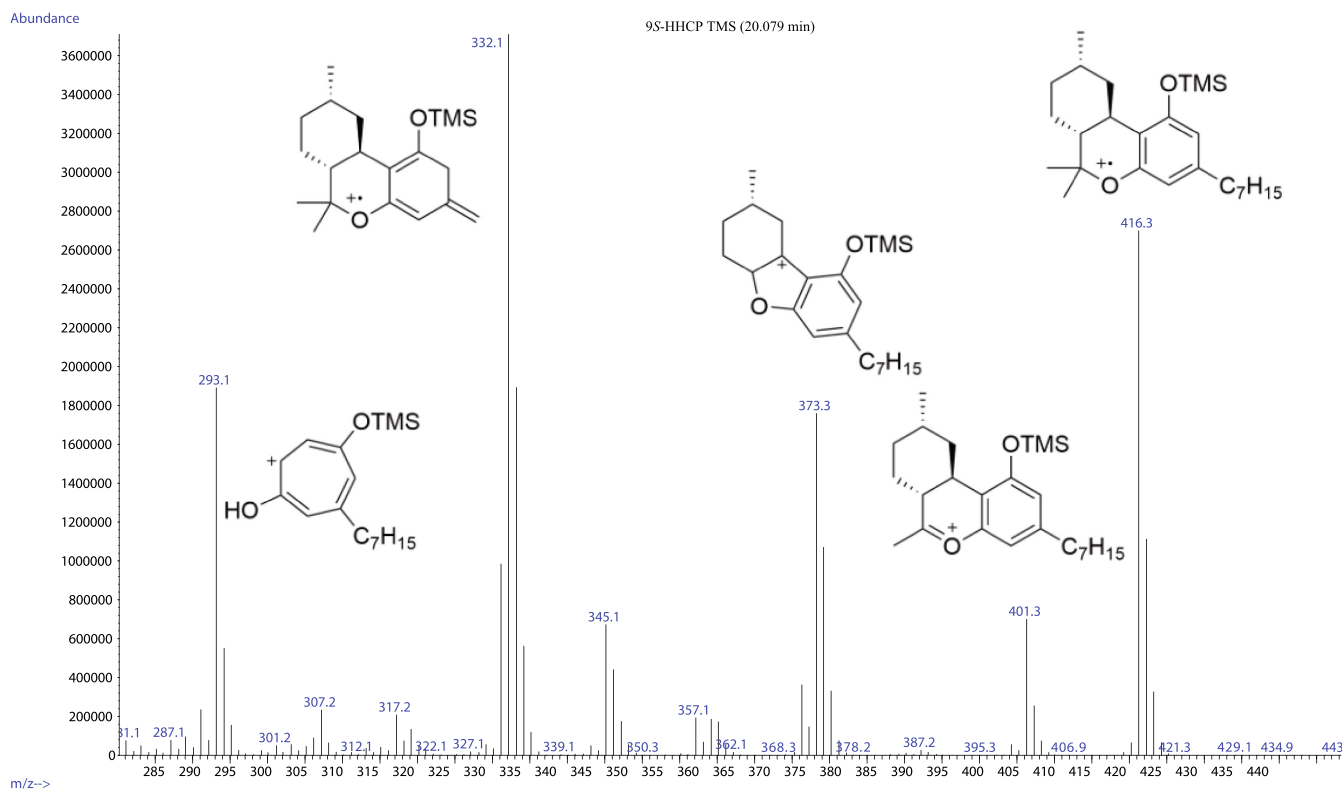


**FIGURE 7** | EI mass spectrum of (9S)-HHCP-TMS with the structures of the most abundant ions. The same fragmentation patterns as in underivatized HHCP are suggested.

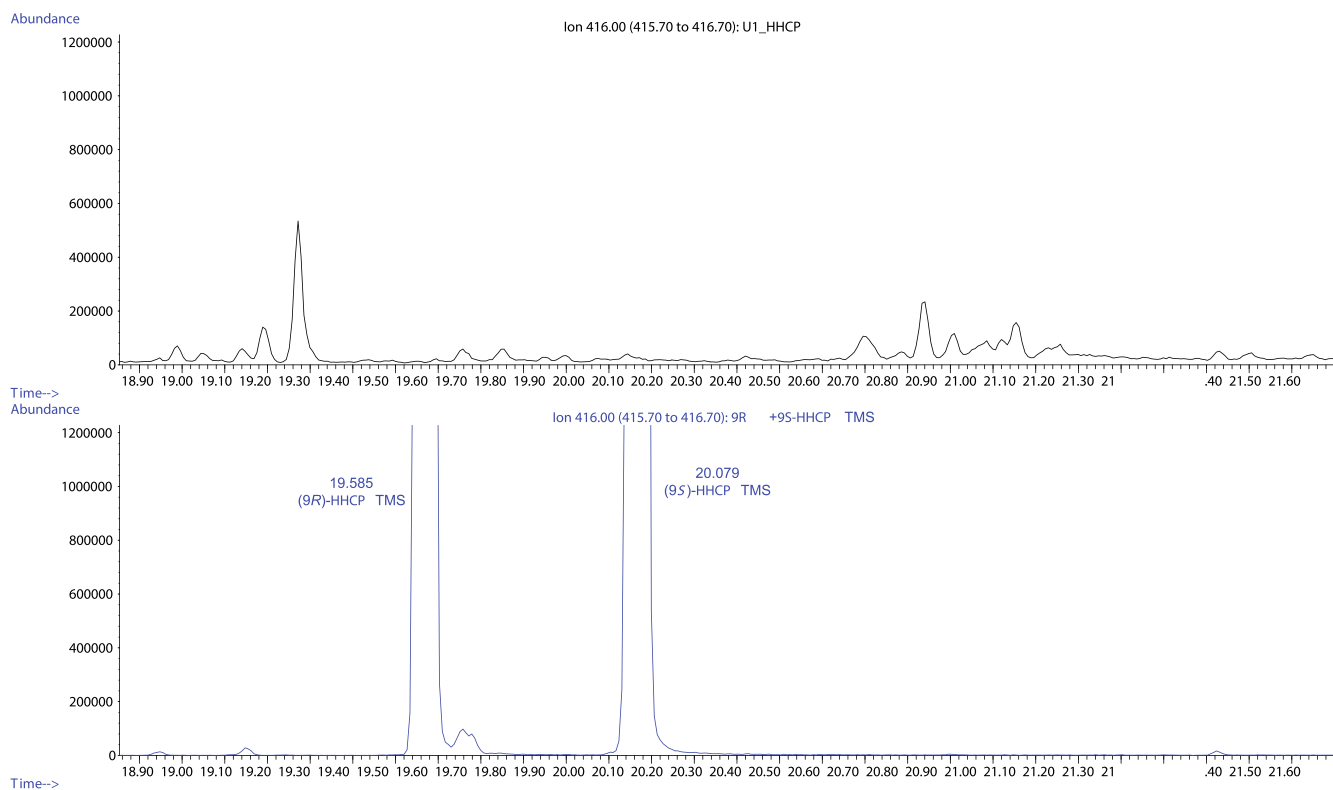


**FIGURE 8** | Stacked XICs ( $m/z$  416) of a reference solution containing (9R)- and (9S)-HHCP-TMS (bottom) and a trimethylsilylated urine sample 10h after oral ingestion of 4-mg HHCP (top). No HHCP-TMS is seen in the urine sample.

## 2.7 | GC–MS of Monohydroxylated Metabolites

Extracted ion chromatogram of  $m/z$  504 showed an intense peak at 21.83 min (see Figure S31). The corresponding spectrum is found in Figure S32. This molecule is presumably a hydroxylated HHCP (2xTMS). The mass spectrum shows characteristic fragments, which are shown in Figure S40. The molecular ion ( $m/z$  504) forms the base peak. Elimination of a methyl radical ( $m/z$  489) is present but of low intensity. The ion resulting from the McLafferty rearrangement is of a quite high abundance ( $m/z$  420). A chromenylium ion ( $m/z$  371) and a tropylium ion ( $m/z$  293) with high intensity are present. The tropylium ion shows that the molecule had no hydroxyl group at the side chain. These fragments can be tentatively assigned to a structure using the spectra of monohydroxylated HHC TMS derivatives [21]. The ions and their relative abundances are similar to the respective ions of the TMS derivative of (9R)-11-OH-HHC. The ion from the McLafferty rearrangement remains the same ( $m/z$  420). The other ions are shifted by  $m/z$  28 due to a longer alkyl chain. This metabolite is therefore tentatively identified as (9R)-11-OH-HHCP.

## 2.8 | GC–MS of Bishydroxylated Metabolites

In contrast to HHC, a significant amount of HHCP is bishydroxylated. Two metabolites were identified that are likely bishydroxylated HHCP as shown in Figure S33 (their spectra are found in Figures S34 and S35). These two compounds show the ions  $m/z$  420 from the McLafferty rearrangement indicating that the alicyclic moiety is monohydroxylated. In addition, the tropylium ions  $m/z$  381 and its fragment ion  $m/z$  291, which forms after the loss of TMSOH, are present. This indicates that there is a hydroxylation position on the side chain as well. The formation of the ions  $m/z$  449 and  $m/z$  562 is unknown. Extracted ion chromatograms of the appearing ions show that these ions coelute with the characteristic ions. The characteristic ions of the trimethylsilyl ethers of bishydroxylated HHCP are shown in Figure S41.

Retention times, Kováts indices, and the relevant ions of the trimethylsilyl ethers of HHCP and their detected metabolites are summarized in Table 2. A chromatogram of the *n*-alkane

**TABLE 2** | Chromatographic data and relevant ions of the TMS derivatives of HHCP and their metabolites.

Name	RT (min)	RRI	Relevant ions (Da)
(9R)-HHCP-TMS	19.58	2546	416, 401, 373, 332, 293
(9S)-HHCP-TMS	20.08	2610	416, 401, 373, 332, 293
HHCP-OH 2xTMS	21.82	2850	504, 420, 371, 293
HHCP-2xOH 3xTMS	23.15	3029	592, 562, 420, 291
HHCP-2xOH 3xTMS	23.51	3072	592, 449, 420, 381, 291

Abbreviations: RRI: relative retention index (Kováts index), RT: retention time.

standard (C7–C40) used for the calculation of the Kováts indices is found in Figure S36.

## 3 | Discussion

No cross-reactivities were observed from the urinary metabolites in the immunoassay for  $\Delta^9$ -THC-COOH. This is in contrast to the human metabolites of HHC which show positive results in urine [10–15], whole blood [24], serum [11], and saliva [11]. (9S)-HHCP and (9R)-HHCP were only found in small amounts in urine after consumption, which indicates a strong metabolic degradation. It is however unlikely that the small amount of HHCP epimers are responsible for the negative immunoassay results. Their cross-reactivity in THC immunoassays is rather weak [13, 16, 25].

The HHCP sample, which was consumed in this study, was previously characterized, and it was found that in addition to (9R)-HHCP and (9S)-HHCP, other regioisomers and stereoisomers were present [9]. These isomeric compounds are probably metabolized in a similar way. It is therefore not clear whether any of the metabolites described originate from the metabolism of an impurity in the recreational HHCP product. However, most of the impurities in the HHCP product are present in very small quantities.

No carboxylic metabolites were found in urine after a single consumption of 4-mg HHCP. This is in accordance with the very low amount of 11-nor-9-carboxy-HHC in urine found after a single oral dose of 20-mg HHC [10]. This is also consistent with a study in which the hepatic metabolites of  $\Delta^9$ -tetrahydrocannabinol ( $\Delta^9$ -THCP) were analyzed in mice. The study showed that hepatic metabolites of  $\Delta^9$ -THCP in mice were mainly hydroxylated compounds containing one to four hydroxyl groups. In contrast to  $\Delta^9$ -THC, carboxy metabolites of  $\Delta^9$ -THCP were present only in small amounts, although THCP has allylic positions that can be easily hydroxylated in vivo [26].

Polyhydroxylated metabolites of  $\Delta^9$ -THC in human are known, but they are only found in small amounts [27, 28]. Only recently, Lindbom et al. reported on bishydroxylated metabolites of HHC in urine samples and in incubation experiments with HHCP using human hepatocytes [17].

The excessive metabolism of HHCP makes it difficult to prove consumption as the parent drug might not be present in urine samples. It is assumed that HHCP (LC-QqTOF and LC-QqLIT) and HHCP-TMS (GC–MS) have a low sensitivity under the measurement conditions used. The same observation was made in a similar experiment in which HHC was consumed. HHC glucuronide was easily detectable using LC–MS, but after deglucuronidation of the urine sample, HHC was barely detected [10]. No forensic markers for HHCP are established yet. Side-chain hydroxylated metabolites seem to be important forensic markers for saturated semisynthetic cannabinoids like HHC and HHCP [10, 14, 17].

In comparison to the recent study on the metabolites of (9R)-HHCP from incubation experiments with human hepatocytes, only monohydroxylated and bishydroxylated metabolites or their glucuronides were observed in the urine samples [17]. Differences

between in vitro and in vivo experiments are to be expected. A single small dose of HHCP would also lead to a different metabolic profile than a regular intake of HHCP. This was seen in a similar experiment with HHC where the respective carboxylic acids were only detected at a small level in urine [10]. Whereas urine samples of regular users from other studies have shown positive results for 11-nor-(9R)-carboxy-HHC or 11-nor-(9S)-carboxy-HHC [29, 30]. The carboxy metabolites of HHC were also found in human blood [24, 31]. It was recently shown that the carboxy metabolites of HHC are minor metabolites of  $\Delta^9$ -tetrahydrocannabinol [32].

## 4 | Conclusions

At this stage, it is unclear which of the identified metabolites originate from (9R)-HHCP and (9S)-HHCP. The isomers and unreacted intermediates, which are present in the synthetic sample, are also excreted from the body after metabolism. One can expect that the metabolites of *cis*-HHCP are similar to the metabolites of (9R)-HHCP and (9S)-HHCP. Some of the identified metabolites might also originate from *cis*-HHCP. Composition of isomeric substance are highly dependent on the synthetic route, measures for stereochemical control, and for purification of the HHCP before sale. In order to maximize profit in an unregulated market, it can be expected that these control measures are rather low.

Monohydroxylated and bishydroxylated HHCP and their glucuronides are recommended as forensic markers for HHCP consumption. (9R)-11-OH-HHCP was the only tentatively identified metabolite but not the most abundant. The same metabolites were recommended as forensic markers for HHCP consumption after incubation experiments with human hepatocytes [17]. In addition, it should be noted that due to low cross-reactivity, samples from real cases might show negative results for cannabinoids when tested with immunoassays.

## Acknowledgments

The team of the Forensic Toxicology and Chemistry from the Institute of Forensic Medicine is highly acknowledged for their help, especially to Isabelle Mösch for the quantification of the HHCP product and Dr. Stefan König for the measurements of the LC-QqTOF samples.

## Conflicts of Interest

The authors declare no conflicts of interest.

## Data Availability Statement

The data that support the findings of this study are available in the Supporting Information of this article.

## References

1. I. Ujváry, "Hexahydrocannabinol and Closely Related Semi-Synthetic Cannabinoids: A Comprehensive Review," *Drug Testing and Analysis* 16 (2023): 127–161, <https://doi.org/10.1002/dta.3519>.
2. C. Caprari, E. Ferri, M. A. Vandelli, C. Citti, and G. Cannazza, "An Emerging Trend in Novel Psychoactive Substances (NPS): Designer THC," *Journal of Cannabis Research* 6 (2024): 21, <https://doi.org/10.1186/s42238-024-00226-y>.

3. Schweizerische Eidgenossenschaft, "Verzeichnisse der Betäubungsmittel, Psychotropen Stoffe, Vorläuferstoffe und Hilfschemikalien (Betäubungsmittelverzeichnisverordnung, BetmVV-EDI) vom 30. Mai 2011 (Stand am 9. Oktober 2023)," <https://www.fedlex.admin.ch/eli/cc/2011/363/de>.

4. N. Reiter, K. Linnet, N. Østermark Andersen, et al., "Svær Forgiftning med Semisyntetiske Cannabinoider," *Ugeskrift for Læger* 186 (2024): V04240241, <https://doi.org/10.61409/V04240241>.

5. Y. Iketani, S. Morita, T. Tsuji, et al., "A Case of Acute Intoxication From Sublingually Administering a Liquid Inhalation Product Containing a Marijuana Analogue," *Tokai Journal of Experimental and Clinical Medicine* 49 (2024): 128–132.

6. L. K. Janssens, K. Van Uytvanghe, J. B. Williams, et al., "Investigation of the Intrinsic Cannabinoid Activity of Hemp-Derived and Semi-synthetic Cannabinoids With  $\beta$ -arrestin2 Recruitment Assays—And How This Matters for the Harm Potential of Seized Drugs," *Archives of Toxicology* 98 (2024): 2619–2630, <https://doi.org/10.1007/s00204-024-03769-4>.

7. M. Persson, R. Kronstrand, M. Evans-Brown, et al., "In Vitro Activation of the CB1 Receptor by the Semi-Synthetic Cannabinoids Hexahydrocannabinol (HHC), Hexahydrocannabinol Acetate (HHC-O) and Hexahydrocannabiphorol (HHC-P)," *Drug Testing and Analysis* (2024), <https://doi.org/10.1002/dta.3750>.

8. Drogeninformationszentrum Zürich (DIZ), "Haschisch mit HHCP, HHCP-O,  $\Delta^8$ -THCP und Syntheseverunreinigungen," (2023), <https://www.saferparty.ch/warnungen/haschisch-mit-synthetischem-cannabinoid-231023>.

9. W. Schirmer, I. Gjuroski, M. Vermathen, et al., "Isolation and Characterization of Synthesis Intermediates and Side Products in Hexahydrocannabiphorol," *Drug Testing and Analysis* (2024), <https://doi.org/10.1002/dta.3759>.

10. W. Schirmer, V. Auwärter, J. Kaudewitz, et al., "Identification of Human Hexahydrocannabinol Metabolites in Urine," *European Journal of Mass Spectrometry* 29, no. 5–6 (2023): 326–337, <https://doi.org/10.1177/14690667231200139>.

11. L. Höfner, S. Becker, J. Dreßler, and S. Baumann, "Quantification of (9R)- and (9S)-Hexahydrocannabinol (HHC) via GC-MS in Serum/Plasma Samples From Drivers Suspected of Cannabis Consumption and Immunological Detection of HHC and Related Substances in Serum, Urine, and Saliva," *Drug Testing and Analysis* 16 (2024): 489–497, <https://doi.org/10.1002/dta.3570>.

12. P. Pettersson-Pablo and J. Oxelbark, "LC-MS/MS Analysis of 11-Nor-9-Carboxy-Hexahydrocannabinol (HHC-COOH) and 11-Hydroxy-Hexahydrocannabinol (HHC-OH) for Verification of Hexahydrocannabinol (HHC) Intake," *Scandinavian Journal of Clinical and Laboratory Investigation* 84 (2024): 109–114, <https://doi.org/10.1080/00365513.2024.2333023>.

13. A. Helander, M. Johansson, T. Villén, and A. Andersson, "Appearance of Hexahydrocannabinols as Recreational Drugs and Implications for cannabis Drug Testing—Focus on HHC, HHC-P, HHC-O and HHC-H," *Scandinavian Journal of Clinical and Laboratory Investigation* 84 (2024): 125–132, <https://doi.org/10.1080/00365513.2024.2340039>.

14. F. Pitterl, M. Pavlic, J. Liu, and H. Oberacher, "Insights Into the Human Metabolism of Hexahydrocannabinol by Non-Targeted Liquid Chromatography–High-Resolution Tandem Mass Spectrometry," *Journal of Analytical Toxicology* 48 (2024): 350–358, <https://doi.org/10.1093/jat/bkae022>.

15. J. Guyon, C. Paradis, K. Titier, et al., "Letter to the Editor: The Cannabinoid Consumed Is Not Necessarily the One Expected: Recent Experience With Hexahydrocannabinol," *Cannabis and Cannabinoid Research* 9, no. 5 (2024): e1459–e1461, <https://doi.org/10.1089/can.2023.0154>.

16. A. L. Patton, I. C. Pacheco, J. Z. Seither, et al., "Cross-Reactivity of 24 Cannabinoids and Metabolites in Blood Using the Immunalysis

- Cannabinoids Direct Enzyme-Linked Immunosorbent Assay,” *Journal of Analytical Toxicology* 48, no. 6 (2024): 439–446, <https://doi.org/10.1093/jat/bkae036>.
17. K. Lindbom, C. Norman, S. Baginski, et al., “Human Metabolism of the Semi-Synthetic Cannabinoids Hexahydrocannabinol, Hexahydrocannabinophorol and Their Acetates Using Hepatocytes and Urine Samples,” *Drug Testing and Analysis* (2024), <https://doi.org/10.1002/dta.3740>.
18. W. Schirmer, S. Schürch, and W. Weinmann, “The Identification of Synthetic Impurities in a Vape pen Containing  $\Delta^9$ -Tetrahydrocannabinophorol Using Gas Chromatography Coupled With Mass Spectrometry,” *Psychoactives* 3, no. 4 (2024): 491–500.
19. N. K. Brown and D. J. Harvey, “*In Vivo* Metabolism of the Methyl Homologues of Delta-8-Tetrahydrocannabinol, Delta-9-Tetrahydrocannabinol and *abn*-Delta-8-Tetrahydrocannabinol in the Mouse,” *Biomedical & Environmental Mass Spectrometry* 15 (1988): 389–398, <https://doi.org/10.1002/bms.1200150706>.
20. T. B. Vree, “Mass Spectrometry of Cannabinoids,” *Journal of Pharmaceutical Sciences* 66 (1977): 1444–1450, <https://doi.org/10.1002/jps.2600661025>.
21. D. J. Harvey and N. K. Brown, “Electron Impact-Induced Fragmentation of the Trimethylsilyl Derivatives of Monohydroxy-Hexahydrocannabinols,” *Biological Mass Spectrometry* 20 (1991): 292–302, <https://doi.org/10.1002/bms.1200200510>.
22. H. Budzikiewicz, R. T. Alpin, D. A. Lightner, et al., “Massenspektroskopie und Ihre Anwendung auf Strukturelle und Stereochemische Probleme—LXVIII: Massenspektroskopische Untersuchung der Inhaltsstoffe von Haschisch,” *Tetrahedron* 21 (1965): 1881–1888, [https://doi.org/10.1016/S0040-4020\(01\)98657-0](https://doi.org/10.1016/S0040-4020(01)98657-0).
23. D. J. Harvey, “Mass Spectrometry of the Cannabinoids and Their Metabolites,” *Mass Spectrometry Reviews* 6 (1987): 135–229, <https://doi.org/10.1002/mas.1280060104>.
24. R. Kronstrand, M. Roman, H. Green, and M. T. Truver, “Quantitation of Hexahydrocannabinol (HHC) and Metabolites in Blood From DUID Cases,” *Journal of Analytical Toxicology* 48 (2024): 235–241, <https://doi.org/10.1093/jat/bkae030>.
25. A.-S. Derne, E. Pape, J.-Y. Jouzeau, A. Kolodziej, N. Gambier, and J. Scala-Bertola, “Immunological Detection of Hexahydrocannabinol (HHC) in Oral Fluid,” *Drug Testing and Analysis* 16 (2024): 638–640, <https://doi.org/10.1002/dta.3595>.
26. D. J. Harvey, “Identification of Hepatic Metabolites of n-Heptyl-Delta-1-Tetrahydrocannabinol in the Mouse,” *Xenobiotica* 15 (1985): 187–197, <https://doi.org/10.3109/00498258509045349>.
27. S. Agurell, M. Halldin, J. E. Lindgren, et al., “Pharmacokinetics and Metabolism of Delta 1-Tetrahydrocannabinol and Other Cannabinoids With Emphasis on Man,” *Pharmacological Reviews* 38 (1986): 21–43.
28. R. J. Dinis-Oliveira, “Metabolomics of  $\Delta^9$ -Tetrahydrocannabinol: Implications in Toxicity,” *Drug Metabolism Reviews* 48 (2016): 80–87, <https://doi.org/10.3109/03602532.2015.1137307>.
29. G. Kobidze, G. Sprega, E. Montanari, et al., “The First LC-MS/MS Stereoselective Bioanalytical Methods to Quantitatively Detect 9R- and 9S-Hexahydrocannabinols and Their Metabolites in Human Blood, Oral Fluid and Urine,” *Journal of Pharmaceutical and Biomedical Analysis* 240 (2024): 115918, <https://doi.org/10.1016/j.jpba.2023.115918>.
30. A. Di Trana, A. Di Giorgi, G. Sprega, et al., “Disposition of Hexahydrocannabinol Epimers and Their Metabolites in Biological Matrices Following a Single Administration of Smoked Hexahydrocannabinol: A Preliminary Study,” *Pharmaceuticals* 17, no. 2 (2024): 249.
31. S. K. Manier, J. A. Valdiviezo, A. C. Vollmer, N. Eckstein, and M. R. Meyer, “Analytical Toxicology of the Semi-Synthetic Cannabinoid Hexahydrocannabinol Studied in Human Samples, Pooled Human Liver S9 Fraction, Rat Samples and Drug Products Using HPLC–HRMS-MS,” *Journal of Analytical Toxicology* 47 (2023): 818–825, <https://doi.org/10.1093/jat/bkad079>.
32. C. Falck Jørgensen, B. Schou Rasmussen, K. Linnet, and R. Thomsen, “Evidence of 11-Hydroxy-Hexahydrocannabinol and 11-Nor-9-Carboxy-Hexahydrocannabinol as Novel Human Metabolites of  $\Delta^9$ -Tetrahydrocannabinol,” *Metabolites* 13, no. 12 (2023): 1169.

### Supporting Information

Additional supporting information can be found online in the Supporting Information section.